Presence of a Slow Dimerization Equilibrium on the Thermal Unfolding of the 205−316 Thermolysin Fragment at Neutral pH †

2 **AUTHORS**, INCLUDING:

Francisco Conejero-Lara

University of Granada

48 PUBLICATIONS   **748** CITATIONS

Presence of a Slow Dimerization Equilibrium on the Thermal Unfolding of the 205−316 Thermolysin Fragment at Neutral pH†

Francisco Conejero-Lara* and Pedro L. Mateo*

Department of Physical Chemistry, Faculty of Sciences, and Institute of Biotechnology, University of Granada, 18071 Granada, Spain

ABSTRACT: Differential scanning calorimetry and size-exclusion chromatography have been used to characterize the dimerization and unfolding of the 205−316 C-terminal fragment of thermolysin at pH 7.5. We show that the folded fragment dimerizes at low temperature with a moderate affinity and undergoes thermal unfolding according to a $N_2 \rightleftharpoons 2N \rightleftharpoons 2U$ model. This behavior has already been observed at acid pH, where a similar dissociation equilibrium has been found [Azuaga, A., Conejero-Lara, F., Rivas G., De Filippis, V., Fontana, A., & Mateo, P. L. (1995) *Biochim. Biophys. Acta 1252*, 95−102]. Nevertheless, at pH 7.5 the dimerization equilibrium slows down below about 30 °C, with virtually no interconversion between the monomeric and the dimeric states of the fragment. We have studied the kinetics of interconversion between monomer and dimer by size-exclusion chromatography experiments and have shown that a very high energy barrier (83.8 kJ/mol at 26.5 °C) exists between either state. A mathematical analysis of the DSC thermograms on the basis of the proposed model has allowed us to obtain the thermodynamic characterization of the dimerization and the unfolding processes of the fragment and confirms the kinetic parameters obtained in the chromatographic experiments. The thermodynamic functions for the unfolding of the fragment are compatible with some degree of disorder in the structures of both the monomer and the dimer. According to circular dichroism measurements, the dimerization of the fragment seems to be linked to some conformational change in the subunits, most probably due to a rearrangement of the existing secondary-structure elements. This fragment displays several features already observed in folding intermediates, such as the partial disorder of the polypeptidic chain, association processes, and kinetic barriers between different regions in the conformational space.

It is well established that the folding pathways of proteins can occur via one or more intermediates, which can range from relatively unordered, pre-molten globules and molten-globule states to highly ordered, near-native intermediate states (Ptitsyn, 1995, and references therein). These intermediate states sometimes have been well characterized, showing the early-forming persistent structural elements in specific domains of the protein, which later lead to the complete folding of the rest of the chain (Radford et al., 1992; Dobson et al., 1994). Isolated fragments from globular proteins are being widely used as models to provide insight into the folding problem (Vita et al., 1979, 1984, 1989; Fontana, 1990; Chaffotte et al., 1991; Peng & Kim, 1994; Rico et al., 1994; Conejero-Lara et al., 1994). These submolecular domains can provide information about local events which could well be of importance during the folding of the complete polypeptide chain.

In previous studies Fontana and co-workers have isolated and characterized a set of thermolysin fragments, most of them from the C-terminal part of the protein, using mainly circular dichroism (CD)[1] and immunochemical measurements. They have proved that in solution these isolated

fragments fold into a native-like conformation (Vita et al., 1979, 1984, 1985; Dalzoppo et al., 1985; Vita et al., 1989; Fontana, 1990). These studies were initially based on the hierarchic organization of the architecture of the protein predicted by computational analysis of its structure (Rashin, 1981, 1984). The 205−316 C-terminal thermolysin fragment in native thermolysin is composed of four α-helices (235−246, 260−274, 281−296, and 301−312) forming a four-helix bundle, an "Ω-loop" between the 235−246 and the 260−274 helices, and several loops in the 205−234 N-terminal part of the chain (Colman et al., 1972; Holmes & Matthews, 1982). The unfolding of the 206−316 fragment by heat, urea, and GuHCl has been previously studied using spectroscopic techniques by Vita and Fontana (1982), who show that it undergoes a cooperative and reversible thermal transition. More recently, thermal unfolding studies of other C-terminal thermolysin fragments have been reported (Vita et al., 1984; Dalzoppo et al., 1985). As a case in point, the small 255−316 fragment, with three α-helices, behaves as a dimer in solution above a certain concentration (Vita et al., 1989; Conejero-Lara et al., 1994). This dimeric structure has been confirmed with the high-resolution structure determination of the fragment in solution by NMR (Rico et al., 1994). We have found very recently, in a differential

---

* Authors to whom correspondence should be addressed. Telephone: +34-58-243333/1. Fax: +34-58-274258.

---

[1] Abbreviations: CD, circular dichroism; DSC, differential scanning calorimetry; HPLC, high-performance liquid chromatography; NMR, nuclear magnetic resonance; SDS, sodium dodecyl sulfate; SEC, size-exclusion chromatography; GuHCl, guanidine hydrochloride.

scanning calorimetry (DSC) and equilibrium sedimentation study at acid pH, that the 205−316 fragment also shows a dimerization equilibrium of the folded fragment, which thermally unfolds following a two-state process (Azuaga et al., 1995).

In the present work we describe and characterize in detail the dimerization and unfolding of the C-terminal 205−316 thermolysin fragment at pH 7.5, using DSC and size-exclusion chromatography (SEC). We show that the folded fragment dimerizes at low temperature with a moderate affinity and undergoes thermal unfolding according to a $N_2 \rightleftharpoons 2N \rightleftharpoons 2U$ model, although, in contrast to acid pH, the dimerization equilibrium at pH 7.5 becomes very slow at low temperature. Thus we have carried out the SEC characterization of the kinetics of interconversion between monomer and dimer, which has shown the presence of a very high energy barrier between them. The mathematical analysis of the DSC thermograms at different concentrations of the fragment based on the proposed model has allowed us to obtain the thermodynamic characterization of both the dimerization and the unfolding processes of the fragment and has also confirmed the kinetic parameters already obtained by SEC. CD measurements were also made to obtain structural information about the isolated monomeric and dimeric states of the fragment. Overall, the present study illustrates several interesting features of the folding−unfolding properties of this small fragment, which are discussed in terms of their relevance to an understanding of the protein-folding problem.

MATERIALS AND METHODS

Sample Preparation and Chemicals. Thermolysin from *Bacillus thermoproteolyticus rokko* was bought from Sigma (St. Louis, MO). The 205−316 thermolysin fragment was prepared by limited autolysis of thermolysin in the presence of EDTA and further purification by reversed-phase HPLC, as described elsewhere (Fassina et al., 1986; Azuaga et al., 1995). Fragment purity was checked by electrophoresis in the presence of SDS. The purified fragment was lyophilized and stored frozen. Before the experiments, samples were prepared by dissolving the lyophilized fragment in water and dialyzing them overnight against a large volume of the required buffer with two changes in the dialysis bath. Fragment concentrations were determined by absorption measurements using an $\epsilon_{280nm}^{0.1\%}$ coefficient of 0.86 (Vita et al., 1979). All chemicals used for buffer preparations were of analytical grade. Milli-Q water was used throughout.

Differential Scanning Calorimetry. DSC experiments were performed in a computer-interfaced DASM-4 microcalorimeter (Privalov & Potekhin, 1986) equipped with 0.47 mL cells, at heating rates of 2.0, 1.0, or 0.5 K/min. A 20 mM phosphate buffer, 0.1 M NaCl, pH 7.5, was used in all experiments. Fragment concentration was varied between 0.15 and 3.6 mg/mL. The baseline of the instrument was routinely recorded before each experiment. Reversibility of the thermal transitions was tested in a second heating of the samples after cooling from the first scan.

Calorimetric traces were processed using home-made software and also software provided by Dr. E. Freire (Johns Hopkins Univerity, Baltimore, MD). After baseline subtraction and smoothing, the calorimetric traces were corrected for the time response of the instrument according to López-Mayorga and Freire (1987). The temperature dependence of the heat capacity of the 205−316 thermolysin fragment was calculated from the calorimetric records according to Privalov and Potekhin (1986) using a molecular weight of 11 978, as calculated from the sequence of the fragment. Further processing and analysis of the DSC curves will be described in Results.

Size-Exclusion Chromatography. The use of several commercial SEC-HPLC columns to characterize the association of the 205−316 thermolysin fragment was precluded by the observed binding of the fragment to the chromatographic media. The experiments could though be carried out using a 1 × 40 cm column packed with Sephadex G75-SF (Pharmacia-LKB) and equipped with a thermostatic jacket. The column was equilibrated at constant temperature with 20 mM phosphate buffer, 0.1 M NaCl, pH 7.5, at a flow rate of 8 mL/h, and was calibrated with molecular mass standards from Sigma. A plot of the logarithm of the molecular weight of the standards against the elution volume yielded a straight line, which was used to determine the apparent molecular mass of the species present in the chromatographic experiments. Three hundred microliter samples of fragment solution, previously dialyzed against the same buffer, were applied to the column. The absorbance of the eluent was monitored at 280 nm using a Uvicord-1 detector (Pharmacia-LKB) connected to a graphic recorder. The chromatograms were digitalized for further computer processing. The relative population of the species present in each chromatographic experiment was determined by fitting a sum of bell-shaped curves to the chromatograms. Two different types of curves were used in the fitting of the chromatographic peaks, depending upon their suitability: a symmetric Lorentzian curve and an asymmetric log-normal curve. The relative area under each fitted peak gave the population of the corresponding species. The errors in the determination of these populations were estimated from the fittings.

Circular Dichroism. A Jasco-720 instrument equipped with a thermostatic cell was used for CD measurements. Spectra were recorded at 10 °C, with a resolution of 1 nm, using a 0.1 mm cell for the far-ultraviolet wavelength range (between 250 and 185 nm) and a 10 mm cell for the near-ultraviolet range (between 320 and 250 nm). Sample concentration varied between 0.5 and 1 mg/mL. The instrument baseline was recorded immediately before all measurements. Spectra were processed with Jasco software and finally expressed in mean-residue molar ellipticity units.

RESULTS

Differential Scanning Calorimetry. We have monitored the thermal unfolding of the 205−316 thermolysin fragment by DSC at pH 7.5, in 20 mM phosphate buffer, 0.1 M NaCl, and at fragment concentrations of between 0.15 and 3.6 mg/mL. An original calorimetric recording is shown in Figure 1, where the transition corresponding to the thermal unfolding of the fragment appears at about 70 °C. A second scan of the same sample showed some loss in the area of this transition (always less than 25%), most likely due to refolding-competing irreversible processes that may occur at high temperatures after the transition. Nevertheless, the effect of the scan rate on its position and shape was negligible (results not shown). This behavior indicates that the unfolding process is taking place under equilibrium conditions. The high unfolding temperature is remarkable, considering that
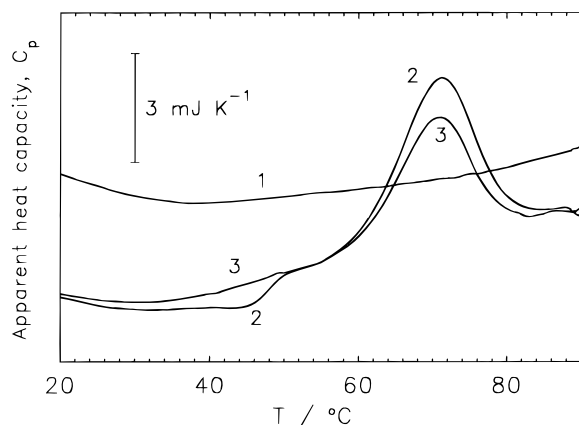
FIGURE 1: Original calorimetric recordings of the 205–316 thermolysin fragment in 20 mM phosphate, 0.1 M NaCl, pH 7.5. The sample concentration was 2.8 mg/mL, and the scan rate was 2.0 K/min. (1) Instrument baseline; (2) first heating of the fragment sample; (3) second consecutive heating of the same sample. The vertical bar indicates the magnitude of the ordinate scale.

the molecule is a protein fragment. This high stability has also been reported for the smaller 255–316 thermolysin fragment under the same experimental conditions (Dalzoppo et al., 1985; Conejero-Lara et al., 1994) as well as for other submolecular domains (Viguera et al., 1994; Azuaga, 1995).

Another interesting feature of the observed thermograms in Figure 1 is the small exothermic pretransition that can be seen around 45 °C, which is not reversible on the second heating of the sample. If the sample is heated just after this exothermic peak and cooled down again, the exotherm is again irreversible on a second scan. This suggests that the irreversibility of this transition is independent of the main unfolding transition. Furthermore, the process responsible for the exothermic transition must be a nonequilibrium one since only endothermic equilibrium processes can be induced by a temperature increase. The kinetic control of this exothermic process was demonstrated when DSC experiments with aliquots from the same sample were made at 0.5, 1, and 2 K/min. A clear decrease in the transition temperature was seen at lower scan rates (results not shown), indicating the time dependence of the process involved. The possibility that this effect was due to the phosphate buffer used in all the experiments was ruled out because DSC experiments in PIPES buffer, at the same pH, gave rise to the same irreversible exothermic transition. The nature of the process responsible for this exothermic effect will be described later.

To obtain the excess heat capacity curves, C_p^{ex}, the chemical baseline has been calculated by tracing sigmoidal curves between the extrapolated C_p lines before the pretransition and after the unfolding transition, as described by Takahashi and Sturtevant (1981). After chemical baseline correction, we have calculated values for the calorimetric increase in enthalpy, ΔH_U^{cal}, and for the van't Hoff enthalpy, $\Delta H_U^{vH} = 4RT_m2C_p^m/\Delta H_U^{cal}$, where C_p^m is the excess heat capacity at the temperature of the maximum of the curves, T_m. The average values are $\Delta H_U^{cal} = 262 \pm 19$ kJ/mol and $\Delta H_U^{vH} = 300 \pm 15$ kJ/mol, which give a value of 0.87 as their ratio. This value is lower than the unit value that might be expected for a two-state monomolecular unfolding process and suggests the presence of a dissociation process accompanying the unfolding of the fragment (Takahashi & Sturtevant, 1981; Freire, 1989), as we have recently reported
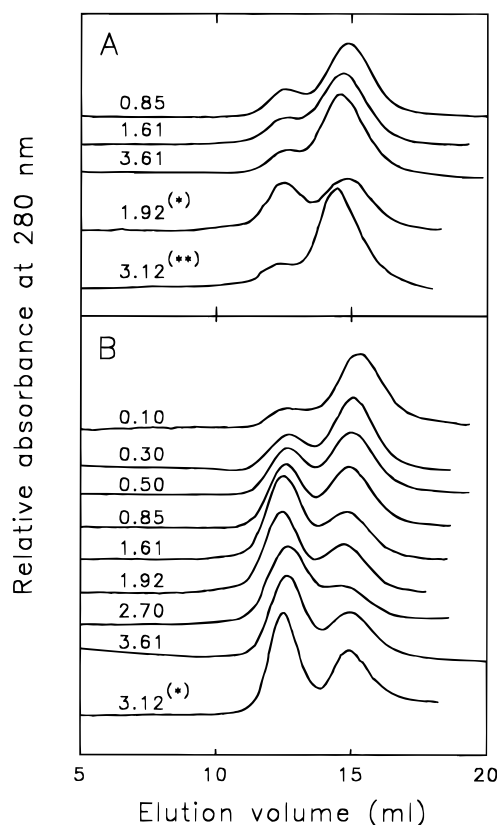

FIGURE 2: Size-exclusion chromatography experiments with the 205–316 fragment in a Sephadex G75-SF column in 20 mM phosphate, 0.1 M NaCl, pH 7.5 and 20 °C. The concentration of the samples is indicated in mg/mL for each elution profile. (A) Samples were prepared by dissolving the lyophilized fragment in water, followed by dialysis overnight at 4 °C against the column buffer; (*) sample dissolved in 6 M GuHCl before the dialysis against the phosphate buffer; (**) similar experiment made in 20 mM PIPES buffer, 0.1 M NaCl, pH 7.5. (B) Samples prepared in phosphate buffer as in the three upper traces in panel A except that before the chromatography runs they were heated to 50 °C for 10 min and then cooled on ice; (*) similar experiment performed in PIPES buffer.

for this fragment at acid pH (Azuaga et al., 1995). The observed increase in the temperature of the maximum of the transitions, T_m, concomitant with sample concentration (see Figure 6) also supports the presence of dimerization equilibrium. This increase is lower than that expected for a two-state, $N_2 \rightleftarrows 2U$ model, the dimeric folded state being N_2 and the unfolded monomer U. An equilibrium model such as $N_2 \rightleftarrows 2N \rightleftarrows 2U$, in which the monomeric and dimeric folded states coexist in equilibrium with the unfolded state during the thermal transition, appears to be a more plausible explanation for the fragment behavior.

Characterization of the Monomer–Dimer Equilibrium by Size-Exclusion Chromatography. We devised SEC experiments under the same buffer conditions as the DSC experiments to characterize the association state of the fragment at low temperature (20 °C). The chromatograms corresponding to samples at several concentrations are shown in Figure 2A. The three upper traces belong to samples dissolved in water and dialyzed overnight at 4 °C against the buffer, in the same way as for the DSC experiments. The fourth trace corresponds to a sample dissolved initially in 6 M GuHCl and then dialyzed against the same pH 7.5 buffer. A similar experiment to the first three, but in PIPES buffer, is also shown in the fifth trace. Two different species

Table 1: Size-Exclusion Chromatography (SEC) Experiments with Samples of the 205−316 Thermolysin Fragment at Different Concentrations, C_t^a

C_t (mg/mL)	V_1 (mL)	V_2 (mL)	M_1	M_2	x_1	x_2	K_D (M × 10⁴)
			Unheated Samples				
0.85	12.60	14.90	21 375	10 938	0.20	0.80	
0.85	12.58	15.20	21 712	10 105	0.22	0.78	
1.61	12.67	14.67	20 950	12 088	0.20	0.80	
3.61	12.60	14.90	21 586	11 030	0.14	0.86	
1.92[b]	12.45	14.85	22 553	11 192	0.39	0.61	
average			21 600 ± 700	11 100 ± 800			
			Samples Heated at 50 °C for 10 min before the SEC Experiment				
0.10	12.66	15.32	21 212	9758	0.15	0.85	0.797
0.30	12.65	15.09	21 273	10 435	0.29	0.71	0.855
0.50	12.62	15.05	21 460	10 557	0.34	0.66	1.076
0,85	12.53	14.93	21 590	10 938	0.42	0.58	1.130
1.61	12.46	14.83	22 026	11 160	0.55	0.45	0.959
1.92	12.42	14.75	22 751	11 524	0.56	0.44	1.132
2.70	12.71	14.81	20 904	11 323	0.61	0.39	1.132
3.61	12.70	14.95	21 586	10 870	0.55	0.45	2.247
average			21 600 ± 600	10 800 ± 600			1.2 ± 0.5

^{a} Experimental conditions are described in the text. Retention volumes (V_1 and V_2), apparent molecular masses (M_1 and M_2) and relative population (x_1 and x_2) of the two species are indicated. The dissociation constant, K_D, is calculated as described in the text. ^{b} Sample prepared by dissolving the lyophilized fragment in 6 M GuHCl and then dialysis against phosphate buffer.

elute from the column, the apparent molecular masses of which correspond very well with the masses of the dimer and the monomer of the fragment (Table 1). Three main conclusions arise from these results: First, at low temperatures the state of the thermolysin fragment corresponds to a mixture of monomers and dimers. Secondly, these two states cannot reach equilibrium at 20 °C due to slow interconversion kinetics since they can be separated by chromatography into individual peaks. This conclusion is also confirmed by the fact that sample concentration has almost no effect on the populations of monomers and dimers; the opposite would be true if there were significant interconversion between them during the experiment. Thirdly, the relative populations of monomers and dimers depend critically upon the way the sample is prepared (see Table 1).

In contrast with these results, the DSC experiments described above show that the unfolding transition occurs under equilibrium, and therefore the monomer−dimer equilibrium should already be established at the unfolding temperatures. The irreversible exothermic transition observed in the DSC thermograms seems to be related to the evolution of the system upon heating from the low-temperature, far-from-equilibrium, frozen state of the system to the high-temperature, rapid equilibrium between monomer and dimer (see below). This slow-to-fast kinetic change appears to end at around 50 °C.

We also performed SEC experiments with samples of different fragment concentrations, which were prepared in the same way as before, except that before loading them into the column they were heated to 50 °C for 10 min and then cooled on ice. The chromatograms thus obtained at 20 °C are shown in Figure 2B for several sample concentrations. Longer heating times did not modify these SEC results. Again, all the chromatograms show two separate peaks, corresponding to the dimer and the monomer of the fragment (see bottom part of Table 1). These results suggest that, after heating to 50 °C and then cooling quickly, the system is not in equilibrium either, since both populations can also be separated by chromatography. In this case, however, the monomer and dimer populations depend closely upon the

sample concentration for each experiment (Table 1). If we assume that a rapid monomer−dimer equilibrium, $N_2 \rightleftharpoons 2N$, is reached on heating to 50 °C, and that the relative populations then become frozen on fast cooling below 20 °C, we can calculate the dimerization equilibrium constants at 50 °C for each experiment according to the equation $K_D = 2C_t x_{N}2/x_{N2}$, where K_D is the dissociation equilibrium constant, x_N and x_{N2} the populations of monomer and dimer, respectively, and C_t the total fragment concentration in (mol of monomer)/L. The values calculated for K_D (Table 1) compare very well for the different sample concentrations, which confirms that equilibrium was established. The average value for K_D is (1.2 ± 0.5) × 10^{-4} M at 50 °C, which corresponds to a moderate affinity for the dimerization of the fragment. These results indicate, therefore, that the slowness of the dimerization process at low temperature is an intrinsic property of the fragment under our experimental conditions. Accordingly, a high-energy barrier must exist at low temperatures between the two states of the fragment, which precludes their fast interconversion.

Now it is clear that the small exothermic peak observed in the DSC thermograms corresponds to the acceleration of the dimerization process caused by the temperature increase, the system coming from a metastable state with a far-from-equilibrium, high-monomer population to the equilibrium populations corresponding to the K_D value. The DSC curves also show that the association process of monomers is exothermic at around 40 °C, i.e., the dissociation enthalpy, ΔH_D, is positive at this temperature.

Characterization of the Kinetics of Monomer Association by Size-Exclusion Chromatography. Fragment samples at a concentration of approximately 2.5 mg/mL were incubated at the desired temperature in a temperature-controlled bath to allow the fragment to dimerize. At measured intervals the interconversion was quenched by rapid cooling on ice. The monomer and dimer populations were determined by SEC as described above. An unheated sample was also analyzed to determine the populations at $t = 0$. The selected temperatures were 35, 37.5, 40, 42.5, and 45 °C. The result of the experiment at 35 °C is shown in Figure 3.
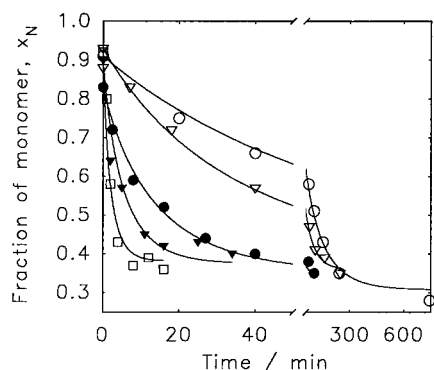
FIGURE 3: Kinetics of the dimerization of the 205−316 thermolysin fragment in phosphate buffer at pH 7.5 with a sample concentration of 2.5 mg/mL. Time dependence of the monomer population at different temperatures: (○) 35.0, (▽) 37.5, (●) 40.0, (▼) 42.5, and (□) 45.0 °C. Symbols correspond to the experimental data calculated from the chromatograms, as described in Materials and Methods. Solid lines correspond to the best fittings according to eq 2 of the Appendix.

We developed the following kinetic model to analyze the data:

$$N_2 \underset{k_2}{\overset{k_1}{\rightleftharpoons}} 2N$$
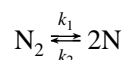
where we assumed that at the temperatures involved the thermal unfolding had not started. k_1 and k_2 are the kinetic constants for dissociation and association respectively. The mathematical derivation of the equations of the model are shown in the Appendix, where an analytical equation (eq 2) for the time dependence of monomer population at constant temperature is obtained. This equation has been used to fit the kinetic curves of the model to the experimental data.

Plots of the experimental values of x_N versus time are shown in Figure 3 for the different temperatures, together with the best fittings, which provided the k_1 and k_2 values for each temperature. In addition, the value for the equilibrium dissociation constant, K_D, at each temperature can be obtained from the relation $K_D = k_1/k_2$. The errors in the values for k_1, k_2, and K_D were estimated by an analysis of the variance of the fittings according to Bevington (1969).

The values of the kinetic constant, k_2, for the association process obtained at several temperatures allow us, through an Arrhenius-type plot, to obtain the activation enthalpy characterizing the transition state between the monomer and the dimer (see Appendix). The plot for k_2 is shown in Figure 4A. The value obtained for the activation enthalpy of the association process, $\Delta H^{\neq}_2$, is 292 ± 24 kJ/(mol of dimer), which is a very high value, close to the unfolding enthalpy of the fragment at the temperatures at which the kinetics was measured [see below and Azuaga et al. (1995)]. This result suggests that the relevant transition state for the dimerization process has the characteristics of a highly disordered state, with a low number of fixed tertiary contacts. From this analysis the temperature at which k_2 equals 1 M^{-1} min^{-1}, T_2, turns out to be 26.5 ± 1.1 °C.

These experiments also provide the temperature dependence of the dissociation constant K_D. We also made equilibrium experiments at several other temperatures by incubating the samples long enough to reach the equilibrium. A plot of ln K_D versus $1/T$ is shown in Figure 4B, from which it should in principle be possible to derive the thermodynamic parameters of the dimerization process (see Appendix).
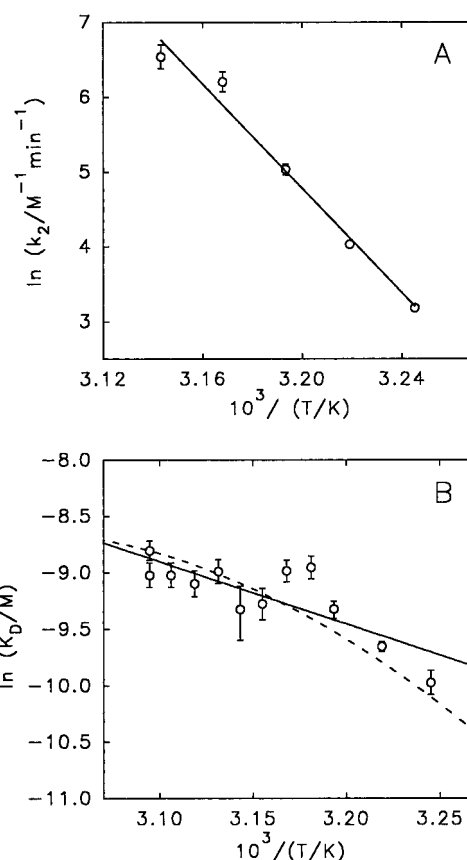

FIGURE 4: Temperature dependence of the kinetic and equilibrium constants for the dimerization of the 205−316 fragment. (A) Plot of ln k_2 versus $1/T$. Symbols correspond to the values of the kinetic dimerization constant, k_2, in M^{-1} min^{-1}, obtained from the fittings shown in panel B. The solid line corresponds to the best fitting to eq 3 of the Appendix. (B) Plot of ln K_D versus $1/T$. Symbols correspond to the values of the equilibrium dissociation constant, K_D, in molar units, obtained from the kinetic experiments shown in Figure 3, as well as from equilibrium experiments at several other temperatures (see text). The solid line represents the best fitting according to eq 4 of the Appendix, assuming $\Delta C_{pD} = 0$. The dashed line corresponds to the temperature dependence of K_D calculated with the same equation by using the parameters of Table 2 obtained from the analysis of the DSC data.

Nevertheless, as can be seen in the figure, the variation of K_D versus temperature is too small compared to the experimental errors to obtain accurate values for the thermodynamic functions. Some preliminary observations can still be derived from the analysis of the K_D values. A zero value for the heat capacity change on dissociation, ΔC_{pD}, predicts a straight line for the plot in Figure 4B, but in fact the experimental data seem to follow a rather curved function of the form shown in the figure, which would be predicted by eq 4 in the Appendix if ΔC_{pD} were negative. This negative ΔC_{pD} value will be confirmed later by an analysis of the DSC data. According to the slope of the curved plot, the dissociation enthalpy, ΔH_D, is positive over the temperature range of our experiments, which agrees with our DSC results.

Simple Model To Explain the DSC Curves of the 205−316 Thermolysin Fragment at pH 7.5. We have developed a mathematical model to explain the observed DSC curves of the 205−316 thermolysin fragment. We observed some irreproducibility in the DSC traces before and after the transitions. This problem precluded a rigorous DSC analysis using the partial heat capacity curves. To make the analysis simpler, the C_p curves have been corrected by a sigmoidal
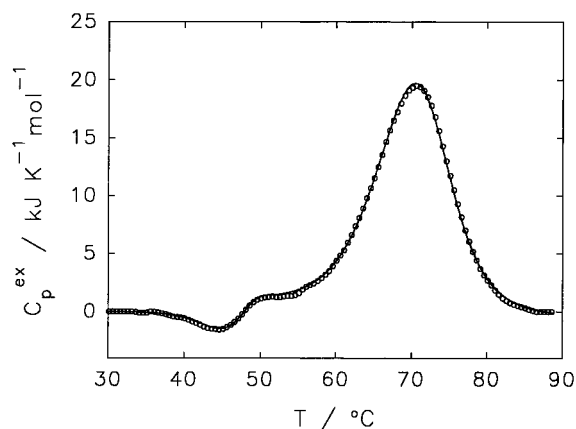
FIGURE 5: Excess-heat-capacity curve for the 205–316 fragment at pH 7.5, after making the chemical baseline correction as described in the text. Sample concentration was 2.84 mg/mL, and the scan rate was 2.0 K/min. Symbols correspond to experimental data. The solid line corresponds to the best fitting according to the equations of the model described in the text.

chemical baseline as described above. This correction eliminates the information about the increment of heat capacity of unfolding, ΔC_{pU}, from the DSC traces. Nevertheless, the value for this magnitude, 4.1 kJ/(K·mol), has been recently determined at acid pH (Azuaga et al., 1995). A corrected DSC thermogram is shown in Figure 5.

The simplest model to describe the system over the whole temperature range i

$$N_2 \underset{k_2}{\overset{k_1}{\rightleftharpoons}} 2N \overset{K_U}{\rightleftharpoons} 2U$$
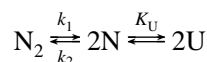
where k_1 and k_2 are the individual kinetic constants of the dimerization process and K_U is the equilibrium unfolding constant. The equilibrium dissociation constant, K_D, is equal to k_1/k_2. The mathematical elaboration of this model is shown in Appendix, where a set of equations is derived to analyze the DSC data. With these equations we have developed specific software to make the fittings to the experimental excess heat capacity, $C_p^{ex}(T)$, curves. Initially, we made the fittings to each individual curve, taking into account the sample concentration, C_t, the scan rate, v, and an initial monomer population, x_{N0}, estimated from the SEC experiments of unheated samples. We also fixed the value for K_D at 50 °C, as obtained from the chromatography experiments. In addition, we split in the value of ΔH_U in eq 9 into two different parameters (Privalov & Potekhin, 1986): ΔH^{cal}, which is the value corresponding to the unfolding transition area, and ΔH^{vH}, the value controlling the temperature dependence of the unfolding equilibrium constant, K_U. Both values must coincide if the unfolding

step is a two-state cooperative transition, as actually happens according to our results.

An example of the individual fittings to the DSC curves is shown in Figure 5, where it is evident that the C_p^{ex} curves are very well described by the equations of the model. The exothermic pretransition before the unfolding transition is also predicted, which supports the idea that it corresponds to the kinetic dimerization of the metastable monomer. The model also predicts the absence of any exothermic peak when the starting monomer and dimer populations are close to the equilibrium ones at temperatures where the heating is initiated in a DSC experiment (results not shown) and also explains the irreversibility of the exothermic process on a second heating of the sample.

The sets of parameters resulting from the individual fittings are shown in Table 2, together with their average values. The parameters describing each curve for different sample concentrations almost coincide, indicating the validity of the model to describe all the experimental data. This result could not have been achieved if we had assumed a zero value for ΔC_{pD}, since in this case the individual fittings resulted in a very different set of values for their characteristic parameters. A negative value for ΔC_{pD} resulted from the fittings, which has already been reported for the thermal unfolding of this thermolysin fragment at acid pH (Azuaga et al., 1995).

To refine the fitting process as much as possible, the average set of parameters was used as input to make a multidimensional fitting to all the DSC curves obtained at different concentrations. The parameters resulting from this fitting, which are very similar to the average ones from the individual fittings, are also shown in Table 2.

The kinetic parameters, $\Delta H^{\neq}_2$ and T_2, obtained from the DSC data and those resulting from the kinetic experiments by SEC (see above) coincide very well. The agreement between the temperature dependence of the dissociation constant measured by chromatography and that predicted by the fitting of the DSC curves is not so good (Figure 4B), but here the errors in K_D are relatively high when compared with the absolute variation of its value with temperature.

As expected, ΔH^{cal} and ΔH^{vH} coincide very well (Table 2), the unfolding enthalpy being about 275 kJ/mol. The experimental and predicted effects of the sample concentration on the temperature of the maximum of the unfolding transitions, T_m, also agree satisfactorily (Figure 6). Finally, it should also be mentioned that the model predicts well the observed dependence of the position of the exothermic dimerization transition both with the scan rate of the DSC experiment and with the sample concentration, as expected for a bimolecular process (results not shown). Therefore, we can conclude that the proposed model describes the thermal unfolding of the 205–316 thermolysin fragment at

Table 2: Thermodynamic Parameters for the Dissociation and Unfolding of the 205–316 Thermolysin Fragment Resulting from the Fitting of the C_p^{ex} Curves Obtained at Different Sample Concentrations, C_t, Using the Equations of the Model as Described in the Text

C_t (mg/mL)	v (K/min)	$\Delta H_D{}^a$	$\Delta C_{pD}{}^b$	$\Delta H_2^{\neq}{}^a$	T_2 (°C)	$\Delta H^{vH\ c}$	$T_{1/2}$ (°C)	$\Delta H^{cal\ c}$
1.01	2.0	38.2	−5.5	289	34.6	286	67.8	284
1.33	2.0	55.2	−3.9	386	31.4	277	68.8	265
1.53	0.5	22.8	−5.7	262	25.6	266	66.8	261
1.69	2.0	49.4	−6.3	319	28.2	272	67.8	295
1.78	2.0	63.6	−4.5	297	27.6	260	68.8	284
2.84	2.0	41.4	−4.7	346	29.9	271	67.7	268
average		45 ± 14	−5.1 ± 0.9	317 ± 44	30 ± 3	272 ± 9	68.0 ± 0.8	276 ± 13
multiple fit		38	−4.4	292	27.7	273	67.8	282

[a] kJ/(mol of dimer). [b] kJ/(K·mol of dimer). [c] kJ/(mol of monomer). ΔH_D values correspond to 50 °C.
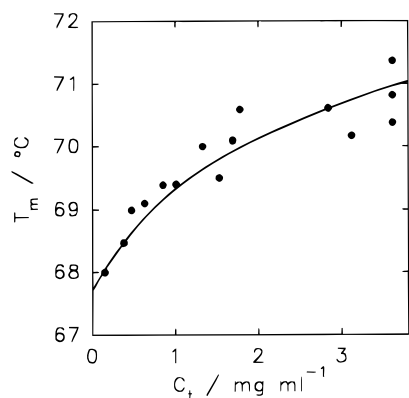
FIGURE 6: Dependence of the temperature of the maximum, T_m, of the excess heat capacity curves with sample concentration. Symbols correspond to experimental values. The solid line shows the dependence predicted by the model described in the text.
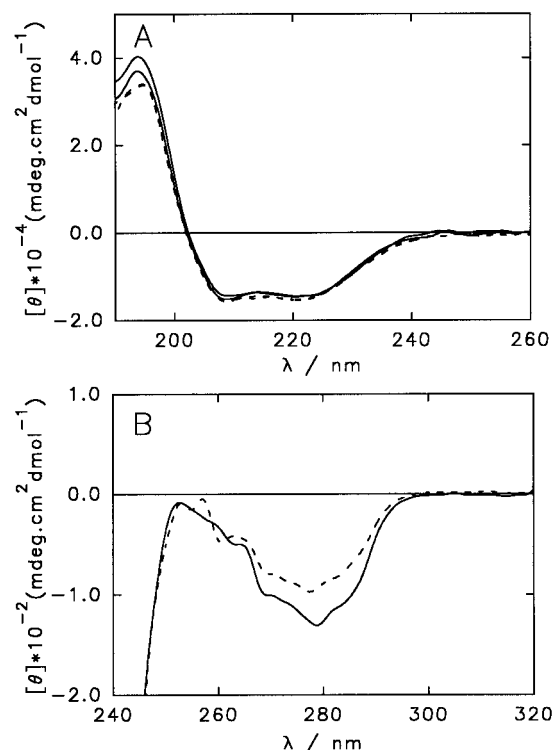

FIGURE 7: Circular dichroism spectra of the monomeric and the dimeric states of the 205−316 thermolysin fragment at pH 7.5 and 10 °C. Solid and dashed lines correspond to dimer and monomer samples, respectively. (A) Far-ultraviolet CD spectra. Spectra of two different samples for both monomer and dimer are shown, where the former are practically indistinguishable. (B) Near-ultraviolet CD spectra.

pH 7.5 very accurately, making it possible to obtain the different thermodynamic and kinetic parameters involved.

Preliminary Structural Characterization of the Monomeric and Dimeric Species by Circular Dichroism. We made preliminary CD measurements to provide some insight into the possible structural differences between the monomer and the dimer of the fragment. Prior to the CD measurements, samples of the monomer and the dimer were isolated by SEC and kept at 0 °C. Spectra of the separated monomer and dimer at 10 °C, where no appreciable interconversion occurs during our experimental time, are shown in Figure 7 for the far- and near-ultraviolet wavelength range.

Figure 7A shows that very small differences exist between the far-UV CD spectra of either species (only slightly detected around 195 nm). Both spectra correspond very well

to that of a typical α-helical shape, as expected from the known secondary structure of the fragment sequence in native thermolysin (Colman et al., 1972; Holmes & Mathews, 1982) as well as from what has been reported for the very close fragments 206−316 (Vita et al., 1979), 228−316 (Vita et al., 1984), and 255−316 (Dalzoppo et al., 1985). Thus, the secondary structure content seems to change little between the monomeric and the dimeric states of the fragment.

On the other hand, the near-UV CD spectra of the monomer and the dimer are quite different, with a less negative ellipticity signal around 277 nm for the monomer (Figure 7B). Since the 205−316 thermolysin fragment contains 3 phenylalanines, eight tyrosines, and no tryptophan residues, most of the signal at 277 nm can be attributed to the Tyr residues, since the Phe residues give a very low signal at this wavelength. A nonzero CD signal in this wavelength range indicates a nonsymmetric environment for the aromatic residues, which is normally associated with the existence of an ordered tertiary structure in the neighborhood of these residues. Accordingly, the dimer seems to have a higher content of fixed tertiary structure than the monomer.

DISCUSSION

Thermal unfolding of the 205−316 thermolysin fragment at pH 7.5 can be expressed according to a model in which the folded monomers and dimers are in equilibrium with each other and undergo reversible unfolding, yielding a monomeric unfolded state. The fact that this fragment is able to undergo a cooperative transition and is also highly stable adds further support to the idea that certain isolated subdomains from thermolysin may fold independently as cooperative units (Fontana, 1990) and might be related to intermediate steps in the folding of the enzyme.

Values of 4.1 kJ/(K·mol) and 186 kJ/mol were obtained for ΔC_{pU} and ΔH_U respectively at 50 °C and acid pH for this fragment, which led to a 268 kJ/mol value for ΔH_U at 70 °C (Azuaga et al., 1995). This agrees closely with the value reported here at pH 7.5 (Table 2). According to Azuaga et al. (1995), the unfolding enthalpy and heat-capacity functions are consistent with a noncompact or partially disordered structure for the fragment (Privalov, 1979) in both monomeric and dimeric states, which seems also to be the case at pH 7.5, although some differences may exist, as will be discussed later.

Monomers and dimers of this fragment are always in rapid equilibrium at acid pH (Azuaga et al., 1995). The dissociation constants for the fragment at pH 7.5 are similar to those reported at acid pH, indicating that the association equilibrium depends little upon pH. This finding suggests that the intersubunit interactions are mainly hydrophobic. In an earlier equilibrium sedimentation study Vita et al. (1989) reported that the 206−316 fragment, without the N-terminal methionine of the fragment studied here, behaved as a monomer at 20 °C and pH 7.5. Both fragments are almost identical, and it is very unlikely that the additional Met residue could be responsible for such a discrepancy in behavior between them. Neither should the different ionic strength used by Vita et al. (1989) justify this difference, since the intersubunit interaction does not seem to be electrostatic. The apparent contradiction between both works can, however, be explained by the fact that, as we show here, the dimerization equilibrium of the fragment at pH 7.5 is frozen at temperatures of around 30 °C and below, where the population of each state depends very much upon sample

preparation (see Results). If the sample does not exceed temperatures of 30−35 °C, therefore, the monomer and dimer populations could be very far from equilibrium, thus giving rise to apparently contradictory results.

An analysis of the DSC data has led to our obtaining an estimate of the thermodynamic parameters for the dimerization equilibrium. The value for the dissociation enthalpy, ΔH_D, is around 40 kJ/(mol of dimer) at 50 °C (Table 2) and higher than the value found in the acid pH study, about 8 kJ/(mol of dimer) at the same temperature (Azuaga et al., 1995). The value obtained for ΔC_{pD} is negative, as it is at acid pH, but higher in absolute value at pH 7.5 [−4.4 kJ/K·(mol of dimer) versus −2.3 kJ/K·(mol of dimer)]. Apart from the errors in these parameters, their differences might be related to the different behavior of the dimerization process at either acid or neutral pH. This negative value contrasts with the normally observed positive ΔC_p of dissociation for protein−ligand and protein−protein interactions (Sturtevant, 1977; Wiesinger & Hinz, 1987; Ross, 1987). We have reported that this negative ΔC_{pD} value could be an indication of a conformational change concomitant with the dissociation of the dimer, involving a net burial of hydrophobic surfaces upon dissociation (Azuaga et al., 1995), since the exposure of hydrophobic surfaces predominates over the change in polar surface as reflected in the values of ΔC_p for association processes (Spolar & Record, 1994). The high resolution structure for the shorter, closely related 255−316 thermolysin fragment has recently been published (Rico et al., 1994), showing that this small fragment is a tightly packed dimer of native-like folded subunits, as previously predicted by Vita et al. (1989) and Conejero-Lara et al. (1994). The interface between monomers has been shown to be highly hydrophobic, and its topology coincides with the one between the 255−316 fragment and the rest of the protein in native thermolysin. The 205−316 fragment has also been studied very recently by NMR at acid pH (manuscript in preparation), where the fragment behaves as a dimer under the NMR conditions. The study shows that the structure of the dimer is practically the same as that found for the smaller 255−316 fragment, but with the N-terminal part of the chain (205−254) disordered. This is consistent with our proposal of a certain disorder for the fragment according to the thermodynamics of its unfolding.

The most striking result of this study is the high-energy barrier found for the dimerization process of the fragment at pH 7.5. The activation Gibbs energy for dimerization is 83.8 kJ/(mol of dimer) at 26.5 °C. In enthalpic terms, the energy barrier is 292 kJ/(mol of dimer) at around 40 °C, which is very close to the value for the enthalpy change between the unfolded and folded monomeric states at the same temperature [nearly 145 kJ/(mol of monomer) at 40 °C; Azuaga et al., 1995]. This result suggests that the transition state has the characteristics of a highly unfolded state, or at least a state with a very low level of fixed tertiary structure. This energy barrier practically disappears at and below pH 5, where the dimerization equilibrium is rapid at all temperatures. For the 255−316 fragment, which has a similar dimeric structure, this high energy barrier does not exist even at pH 7.5, since rapid dimerization equilibrium is observed (Vita et al., 1989; Conejero-Lara et al., 1994). In this small fragment the association−dissociation between subunits seems to consist of a simple docking between folded subunits, each one formed by three α-helices. For the 205−316 fragment at acid pH, the additional segment of polypep-

tidic chain (205−254) does not seem to play any role in the dimeric structure, since, according to NMR studies, it is essentially disordered. Nevertheless, the 205−254 segment seems to play a role in the association kinetics of the 205−316 fragment at pH 7.5. As this chain is practically unfolded in the dimer below pH 5.0, an increase in its ordering at neutral pH might call for an almost complete unfolding of the whole chain for both association and dissociation. These possible structural differences could be related to the different values found for the thermodynamic functions of the association/dissociation process at pH 7.5 compared to those at acid pH.

The fact that the energy barrier appears between pH 5 and 7.5 suggests that it might be related to histidine deprotonation. The 235−246 α-helix in native thermolysin has a single positively charged residue (Lys239) in its middle part. On both sides of the helix there are two histidine residues (His231 and His250), which should be protonated at acid pH and could produce charge repulsion with Lys239, and possibly other positive charges, thus destabilizing the fold at this part of the chain, as mentioned above. At pH 7.5, on the other hand, the histidine residues would be essentially deprotonated and the electrostatic repulsion should vanish, allowing for a more extended folding of this part of the chain and producing the observed different behavior in terms of the existence of the high energy barrier. Nevertheless, further structural studies of the fragment at pH 7.5 are necessary to check this tentative explanation.

The far-UV CD spectra of isolated monomers and dimers of the fragment indicate little difference in the secondary structure content, with both states showing typical α-helical spectra, in agreement with the secondary structure of the fragment in native thermolysin. The near-UV CD spectra show, however, a significant change in the environment of the aromatic residues. Thus, fragment dissociation does not seem to involve any change in the secondary structure content but probably a reorganization of the existing elements, mainly α-helices.

The study described here with a protein fragment provides valuable information about several issues that are of present interest in the literature: First, the isolated 205−316 thermolysin fragment is able to adopt a folded tertiary structure and undergo cooperative unfolding. Isolated protein fragments are widely used as models for folding intermediates (Wetlaufer, 1981; Fontana, 1990; Peng & Kim, 1994). Our study of the 205−316 fragment at pH 7.5, together with the previous work at acid pH (Azuaga et al., 1995), shows that although it is very probable that most of the native fold remains, its unfolding thermodynamics indicate some degree of disorder in its structure. It is possible that certain parts of the chain lack the necessary determinants to establish the medium- to long-range interactions that stabilize the local conformations resulting from short-range interactions, as has already been seen with a protein fragment (Chaffotte et al., 1991). Nevertheless, the fact that the isolated fragment can spontaneously fold in solution indicates that it might very well correspond to a folding domain of thermolysin (Vita et al., 1979).

Secondly, the fragment forms dimers in solution, with a concomitant stabilization with respect to the monomeric form. Association of folding−unfolding intermediates is a very common observation in both equilibrium (Filimovov et al., 1993; De Felippis et al., 1993; Sanz et al., 1994) and kinetic studies (Eliezer et al., 1993), and it has been attributed

in some cases to very specific interactions (De Felippis et al., 1993). The dimeric structure of the 255−316 thermolysin fragment shows a very hydrophobic interface between the two subunits, which are formed by the three C-terminal α-helices in thermolysin (Rico et al., 1994). The same dimeric fold has been found for the 205−316 fragment at acid pH, the N-terminal part of which is disordered, and it is also very likely that a similar dimeric arrangement is conserved at pH 7.5. These observations indicate that this fragment's behavior might well represent the type of associative events that occur very frequently during the folding of proteins.

Thirdly, there is a high-energy barrier between the monomer and the dimer of the fragment at pH 7.5. The existence of energy barriers in protein folding has been reported previously for α-lytic protease (Baker et al., 1992) and subtilisin BPN′ (Eder et al., 1993), which, in the absence of their respective pro-regions, are trapped in a partially folded intermediate state. The existence of high barriers separating energy minima has been interpreted as a means of kinetically rendering certain regions of the conformational space inaccessible to the polypeptide chain (Baker et al., 1992). In the case of our fragment the existence of the kinetic barrier could be important in the folding mechanism of thermolysin in that it minimizes unwanted associations of folding intermediates, which could well kinetically trap the polypeptide chain into a misfolded conformation.

ACKNOWLEDGMENT

APPENDIX

The mathematical derivation of the equations corresponding to the models described in Results are set out below.

slow dimerization

$$N$$

$$2N \underset{k_2}{\overset{k_1}{\rightleftharpoons}} N$$

The kinetic equation at constant temperature for this model can be written as

$$\frac{dx_N}{dt} = k_1 x_{N_2} - 2k_2 C_t x_N^2 = k_1 - k_1 x_N - 2k_2 C_t x_N^2 \quad (1)$$

where x_N is the fraction of monomers, k_1 and k_2 are the kinetic constants and C_t is the total fragment concentration.

This equation can be integrated to obtain

$$t = \frac{1}{\sqrt{-q}} \log\left[\frac{(2Cx_N + B - \sqrt{-q})(2Cx_{NO} + B + \sqrt{-q})}{(2Cx_{NO} + B - \sqrt{-q})(2Cx_N + B + \sqrt{-q})}\right] \quad (2)$$

where $q = -4BC - B^2$, $B = -k_1$, and $C = -2C_t k_2$.

Equation 2 can be solved recursively to obtain x_N as a function of time for an initial monomer population, x_{N0}, and a sample concentration C_t.

The temperature dependence of k_2 can be described using the following equation:

$$\ln k_2(T) = -\frac{\Delta H_2^{\neq}(T_2)}{R}\left(\frac{1}{T} - \frac{1}{T_2}\right) + \ln\left(\frac{T}{T_2}\right) \quad (3)$$

where $\Delta H^{\neq}_2$ is the activation enthalpy for the association process, i.e., the enthalpy difference between the transition state and the monomer. T_2 is the temperature at which k_2 equals $1 \text{ M}^{-1} \text{ min}^{-1}$.

The temperature dependence of K_D is described by the van't Hoff equation: $d(\ln K_D)/dT = \Delta H_D/RT^2$, which can be integrated to obtain

$$\ln K_D(T) = \ln K_D(T_d) - \frac{\Delta H_D}{R}\left(\frac{1}{T} - \frac{1}{T_d}\right) + \frac{\Delta C_{pD}}{R}\left[\ln\left(\frac{T}{T_d}\right) + \frac{T_d}{T} - 1\right] \quad (4)$$

where ΔH_D and ΔC_{pD} are the enthalpy and heat capacity changes on dissociation respectively, and T_d is a reference temperature.

slow dimerization and unfolding

$$N_2 \underset{k_2}{\overset{k_1}{\rightleftharpoons}} 2N \overset{K_U}{\rightleftharpoons} 2U$$
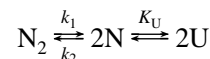
This model describes the behavior of the fragment at temperatures below about 50 °C, where the association−dissociation process is controlled by the individual kinetic constants. In this situation the time dependence of the monomer population, x_N, is given by the kinetic eq 1. Taking into account that $x_N + x_{N2} + x_U = 1$ and $K_U = x_U/x_N$ and introducing the scan rate of the DSC experiment as $v = dT/dt$, we can obtain the temperature dependence of x_N as

$$\frac{dx_N}{dT} = \frac{1}{v}(k_1[1 - x_N(1 + K_U)] - 2k_2 C_t x_N^2) \quad (5)$$

The temperature dependences of the kinetic constants, k_1 and k_2, and of the equilibrium constants, K_D and K_U, are described by the following equations:

$$\frac{d \ln k_1}{dT} = \frac{\Delta H_1^{\neq} + RT}{RT^2}; \qquad \frac{d \ln k_2}{dT} = \frac{\Delta H_2^{\neq} + RT}{RT^2}$$

$$\frac{d \ln K_D}{dT} = \frac{\Delta H_D}{RT^2}; \qquad \frac{d \ln K_U}{dT} = \frac{\Delta H_U}{RT^2} \quad (6)$$

where $\Delta H^{\neq}_1$ and $\Delta H^{\neq}_2$ are the activation enthalpies of the individual kinetic processes. The integrated forms of eq 6 for k_2 and K_D are shown in eqs 3 and 4. For K_U the relevant equation is

$$\ln K_U = -\frac{\Delta H_U}{R}\left(\frac{1}{T} - \frac{1}{T_{1/2}}\right) \quad (7)$$

where $T_{1/2}$ is the temperature at which ΔG_U becomes zero, i.e., the unfolding equilibrium constant is equal to unity. ΔH_U is considered to be constant for the purposes of analyzing

the calorimetric curves, since the contribution of ΔC_{pU} has been eliminated by tracing the chemical baseline as described in Results. This is a reasonable approximation since all our DSC experiments were made at pH 7.5 (the sample concentration alone being varied) and all the unfolding transitions took place at very similar temperatures, with little effect of ΔC_{pU} on ΔH_U. On the other hand, the existence of a heat capacity change on dissociation, ΔC_{pD}, cannot be ignored since the dissociation process occurs over a very wide range of temperatures, and, as described in Results, its effect impinges clearly on the DSC curves.

Equation 5 has to be solved numerically to obtain the temperature dependence of x_N, where we know the initial value of x_N, x_{N0}, the total fragment concentration, C_t, and the heating rate of the DSC experiment, v. Once x_N is known as a function of temperature, we can easily calculate the excess enthalpy, $\langle H\rangle(T)$, taking the folded dimer as the reference state:

$$\langle H\rangle T = \frac{1}{2}\Delta H_D(T)x_N + \left(\frac{1}{2}\Delta H_D(T) + \Delta H_U\right)K_U x_U \quad (8)$$

and the excess heat capacity, $C_p^{ex}(T)$, turns out to be

$$C_p^{ex}(T) = \frac{d\langle H\rangle(T)}{dT} = \left[\frac{1}{2}\Delta H_D + K_U\left(\frac{1}{2}\Delta H_D + \Delta H_U\right)\right]\frac{dx_N}{dT} + \left[\frac{1}{2}\Delta C_{pD}(1 + K_U) + \left(\frac{1}{2}\Delta H_D + \Delta H_U\right)K_U\frac{\Delta H_U}{RT^2}\right]x_N \quad (9)$$

where dx_N/dT is given in eq 5.

Rapid Dimerization and Unfolding. As the temperature increases, so do the values of the kinetic constants until a rapid equilibrium is established. We assumed that rapid equilibrium is reached under our experimental conditions when the values of both k_1 and k_2 are higher than 10^5 min^{-1} and 10^5 M^{-1} min^{-1}, respectively. According to the final fittings, this criterion is achieved at around 50 °C. In this case the model corresponds to

$$2U \underset{K_D}{\overset{N}{\rightleftharpoons}} 2N \underset{K_U}{\overset{}{\rightleftharpoons}} 2U$$

On the other 2U_2 + x_N + x_D = 1 at each temperature, and using the equilibrium constants K_D and K_U it follows that

$$\frac{2C_t}{K_D}x_N^2 + (1 + K_U)x_N - 1 = 0 \quad (10)$$

which can be solved to obtain x_N as a function of temperature:

$$x_N = \frac{1}{C_t}\left(-\frac{K_D}{4} - \frac{K_D K_U}{4} + \sqrt{\frac{K_D^2}{16} + \frac{K_D^2 K_U}{16} + \frac{K_D^2 K_U^2}{16} + \frac{K_D C_t}{2}}\right) \quad (11)$$

The derivative of this equation provides dx_N/dT which for simplicity is not analytically shown. The excess heat capacity curve, $C_p^{ex}(T)$, is once more calculated with eq 9.

REFERENCES

Azuaga, A. (1995) Doctoral Thesis, University of Granada, Spain.

Azuaga, A., Conejero-Lara, F., Rivas, G., De Filippis, V., Fontana, A., & Mateo, P. L. (1995) *Biochim. Biophys. Acta 1252*, 95−102.

Baker, D., Sohl, J. L., & Agard, D. A. (1992) *Nature 356*, 263−265.

Bevington, P. R. (1969) in *Data Reduction and Error Analysis for Physical Sciences*, McGraw-Hill, New York.

Chaffotte, A., Guillou, Y., Delepierre, M., Hinz, H.-J., & Goldberg, M. E. (1991) *Biochemistry 30*, 8067−8074.

Colman, P. M., Jansonius, J. N., & Matthews, B. W. (1972) *J. Mol. Biol. 70*, 701−724.

Conejero-Lara, F., De Filippis, V., Fontana, A., & Mateo, P. L. (1994) *FEBS Lett. 344*, 154−156.

Dalzoppo, D., Vita, C., & Fontana, A. (1985) *J. Mol. Biol. 182*, 331−340.

De Felippis, M. R., Alter, L. A., Pekar, A. H., Havel, H. A., & Brems, D. N. (1993) *Biochemistry 32*, 1555−1562.

Dobson, C. M., Evans, P. A., & Radford, S. E. (1994) *Trends Biochem. Sci. 19*, 31−37.

Eder, J., Rheinnecker, M., & Fersht, A. R. (1993) *Biochemistry 32*, 18−26.

Eliezer, D., Chiba, K., Tsuruta, H., Doniach, S., Hodgson, K. O., & Kihara, H. (1993) *Biophys. J. 65*, 912−917.

Fassina, G., Vita, C., Dalzoppo, D., Zamai, M., Zambonin, M., & Fontana, A. (1986) *Eur. J. Biochem. 156*, 221−228.

Filimonov, V. V., Prieto, J., Martínez, J. C., Bruix, M., Mateo, P. L., & Serrano, L. (1993) *Biochemistry 32*, 12906−12921.

Fontana, A. (1990) in *Peptides: Chemistry, Structure and Biology* (Rivier, J., & Marshall, G. E., Eds.) pp 557−564, Escom, Leiden, The Netherlands.

Freire, E. (1989) *Comments Mol. Cell. Biophys. 6*, 123−140.

Holmes, M. A., & Matthews, B. W. (1982) *J. Mol. Biol. 160*, 623−630.

López-Mayorga, O., & Freire, E. (1987) *Biophys. Chem. 87*, 87−96.

Peng, Z., & Kim, P. S (1994) *Biochemistry 33*, 2136−2141.

Privalov, P. L. (1979) *Adv. Protein Chem. 33*, 167−241.

Privalov, P. L., & Potekhin, S. A. (1986) *Methods Enzymol. 113*, 4−51.

Ptitsin, O. B. (1995) *Curr. Opin. Struct. Biol. 5*, 74−78.

Radford, S. E., Dobson, C. M., & Evans, P. A. (1992) *Nature 358*, 302−307.

Rashin, A. A. (1981) *Nature 291*, 85−87.

Rashin, A. A. (1984) *Biochemistry 23*, 5518−5519.

Rico, M., Jiménez, M. A., González, C., De Filippis, V., & Fontana, A. (1994) *Biochemistry 33*, 14834−14847.

Ross, P. D. (1987) in *Thermodynamic Data for Biochemistry and Biotechnology* (Hinz, H. J., Ed.) pp 227−233, Springer-Verlag, Berlin.

Sanz, J. M., Johnson, C. M., & Fersht, A. R. (1994) *Biochemistry 33*, 11189−11199.

Spolar R. S., & Record, M. T., Jr. (1994) *Science 263*, 777−784.

Sturtevant, J. M. (1977) *Proc. Natl. Acad. Sci. U.S.A. 74*, 2236−2240.

Takahashi, K., & Sturtevant, J. M. (1981) *Biochemistry 20*, 6185−6190.

Viguera, A. R., Martínez, J. C., Filimonov, V. V., Mateo, P. L., & Serrano, L. (1994) *Biochemistry 33*, 2142−2150.

Vita, C., Fontana, A., Seeman, J. R., & Chaiken, I. M. (1979) *Biochemistry 18*, 3023−3031.

Vita, C., & Fontana, A. (1982) *Biochemistry 21*, 5196−5202.

Vita, C., Dalzoppo, D., & Fontana, A. (1984) *Biochemistry 23*, 5512−5518.

Vita, C., Fontana, A., & Chaiken, I. W. (1985) *Eur. J. Biochem. 151*, 191−196.

Vita, C., Fontana, A., & Jaenicke, R. (1989) *Eur. J. Biochem. 183*, 513−518.

Wetlaufer, D. B. (1981) *Adv. Protein Chem. 34*, 61−92.

Wiesinger, H., & Hinz, H. J. (1987) in *Thermodynamic Data for Biochemistry and Biotechnology* (Hinz, H. J., Ed.) pp 211−226, Springer-Verlag, Berlin.